Available online at www.sciencedirect.com
SCIENCE DIRECT®
Journal of Volcanology and Geothermal Research 151 (2006) 365–381
Journal of volcanology and geothermal research
www.elsevier.com/locate/jvolgeores

Sustained long-period seismicity at Shishaldin Volcano, Alaska

Tanja Petersen [a,*], Jacqueline Caplan-Auerbach [b], Stephen R. McNutt [a]

[a] *Alaska Volcano Observatory, Geophysical Institute, University of Alaska Fairbanks, 903 Koyukuk Dr. Fairbanks, AK 99775-7320, USA*
[b] *Alaska Volcano Observatory, USGS Alaska Science Center, 4200 University Dr. Anchorage, AK 99508, USA*

Received 3 March 2005; received in revised form 18 August 2005; accepted 16 September 2005
Available online 21 November 2005

Abstract

From September 1999 through April 2004, Shishaldin Volcano, Aleutian Islands, Alaska, exhibited a continuous and extremely high level of background seismicity. This activity consisted of many hundreds to thousands of long-period (LP; 1–2 Hz) earthquakes per day, recorded by a 6-station monitoring network around Shishaldin. The LP events originate beneath the summit at shallow depths (0–3 km). Volcano tectonic events and tremor have rarely been observed in the summit region. Such a high rate of LP events with no eruption suggests that a steady state process has been occurring ever since Shishaldin last erupted in April–May 1999. Following the eruption, the only other signs of volcanic unrest have been occasional weak thermal anomalies and an omnipresent puffing volcanic plume. The LP waveforms are nearly identical for time spans of days to months, but vary over longer time scales. The observations imply that the spatially close source processes are repeating, stable and non-destructive. Event sizes vary, but the rate of occurrence remains roughly constant. The events range from magnitude ~0.1 to 1.8, with most events having magnitudes <1.0. The observations suggest that the conduit system is open and capable of releasing a large amount of energy, approximately equivalent to at least one magnitude 1.8–2.6 earthquake per day. The rate of observed puffs (1 per minute) in the steam plume is similar to the typical seismic rates, suggesting that the LP events are directly related to degassing processes. However, the source mechanism, capable of producing one LP event about every 0.5–5 min, is still poorly understood. Shishaldin's seismicity is unusual in its sustained high rate of LP events without accompanying eruptive activity. Every indication is that the high rate of seismicity will continue without reflecting a hazardous state. Sealing of the conduit and/or change in gas flux, however, would be expected to change Shishaldin's behavior.

Keywords: Shishaldin volcano; volcano seismology; long-period earthquakes

1. Introduction

In September 1999, a few months after it last erupted (Nye et al., 2002), Shishaldin Volcano, Aleutian Arc, Alaska (Fig. 1), started to exhibit a long-lasting continuous and extremely high level of background seismicity. This consists of many hundreds to approximately two thousand long-period (LP) earthquakes per day (Fig. 2) originating beneath the summit at shallow depths. The unusually high and continuous earthquake rate is 2–3 orders of magnitude higher than that observed at any of the other 26 volcanoes monitored by the Alaska Volcano Observatory (AVO) (Dixon et al., 2003). A high rate of LP seismicity has often been associated with pre-eruptive behavior at many other volcanoes, including Mount Redoubt (Chouet et al., 1994), Galeras Volcano (Gil Cruz and Chouet, 1997), El Chichon (Havskov et al., 1983), and Mount Pinatubo

* Corresponding author. Tel.: +1 907 474 6171.
E-mail address: tanja@giseis.alaska.edu (T. Petersen).

0377-0273/$ - see front matter © 2005 Elsevier B.V. All rights reserved.
doi:10.1016/j.jvolgeores.2005.09.003

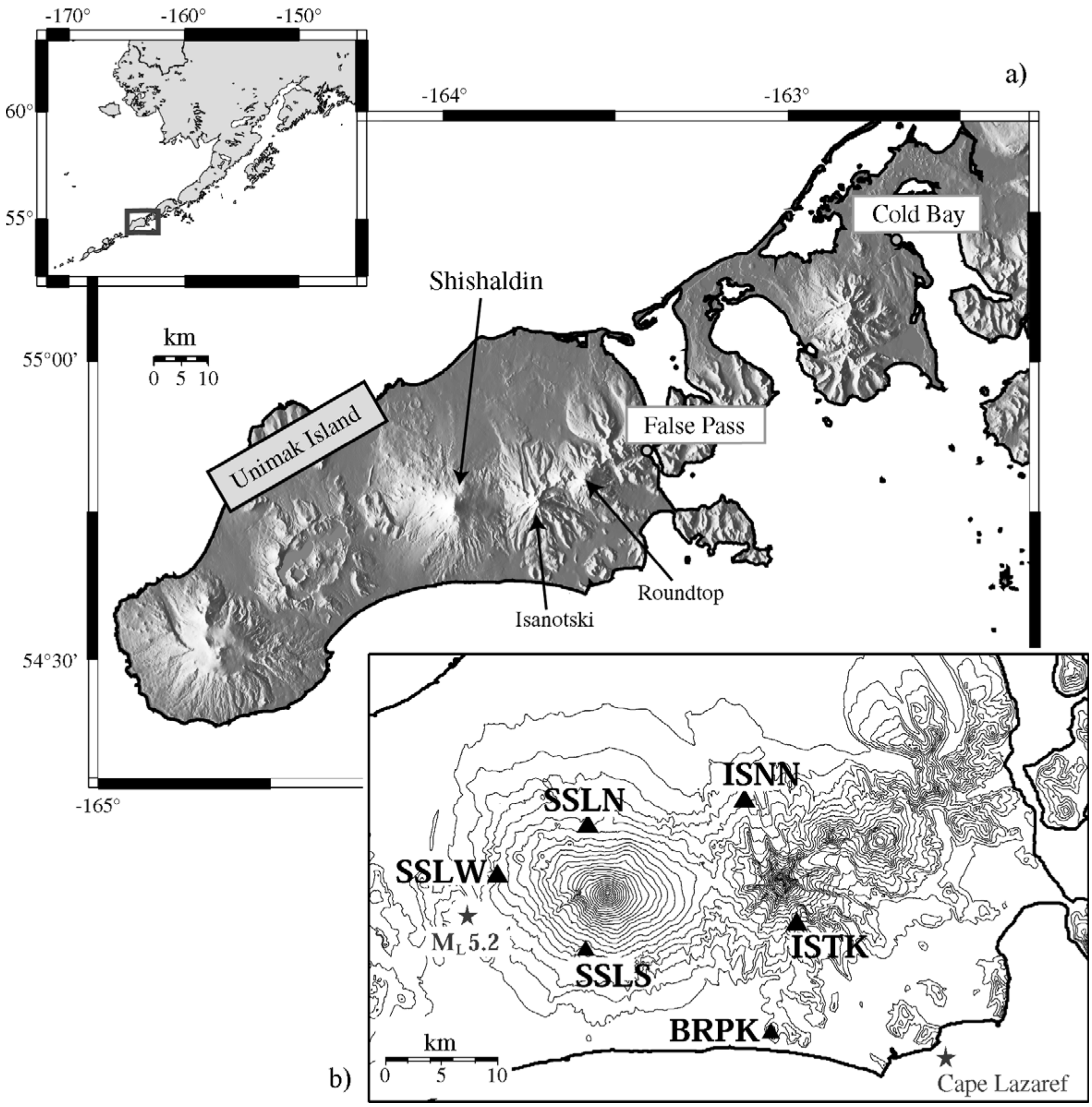

Fig. 1. (a) Map of Unimak Island, easternmost island in the Aleutian Arc, Alaska. False Pass and Cold Bay are the nearest population centers to Shishaldin Volcano. Roundtop and Isanotski volcanoes block the view from False Pass to Shishaldin, but the volcano is visible from Cold Bay. (b) Seismic network around Shishaldin and Isanotski volcanoes. The locations of the six short-period seismometers are marked by triangles. All stations are vertical, short-period (L-4C, 1 Hz) seismometers, except SSLS, which is a three-component L-22 with natural frequency of 2 Hz. The distances of the stations to the summit are: 6.3 km (SSLN), 9.8 km (SSLW), 5.3 km (SSLS), 19.0 km (BRPK), 17.0 km (ISTK) and 14.8 km (ISNN). The pressure sensor is co-located with station SSLN. The area where the M_L 5.2 earthquake and its aftershock sequence are located is indicated by a star. Another cluster area for VT events is located southeast of Isanotski off of Cape Lazaref.

(Harlow et al., 1997). Shishaldin, however, shows no other signs of volcanic unrest except for an omnipresent volcanic plume and occasional weak hotspots in thermal satellite imagery when viewing conditions are optimal. Shishaldin's seismic activity is almost exclusively composed of discrete LP events; volcano tectonic events are rare in the summit region. Another relevant feature of the seismic activity at Shishaldin is the extreme similarity between some of the events over long time scales of up to several months. At the beginning of May 2004, the seismicity radically changed to tremor and the extended earthquake swarm ended. The high rate of LP events over a 4.6-year time period, together with the lack of eruptive behavior makes Shishaldin unusual among volcanoes anywhere in the world.

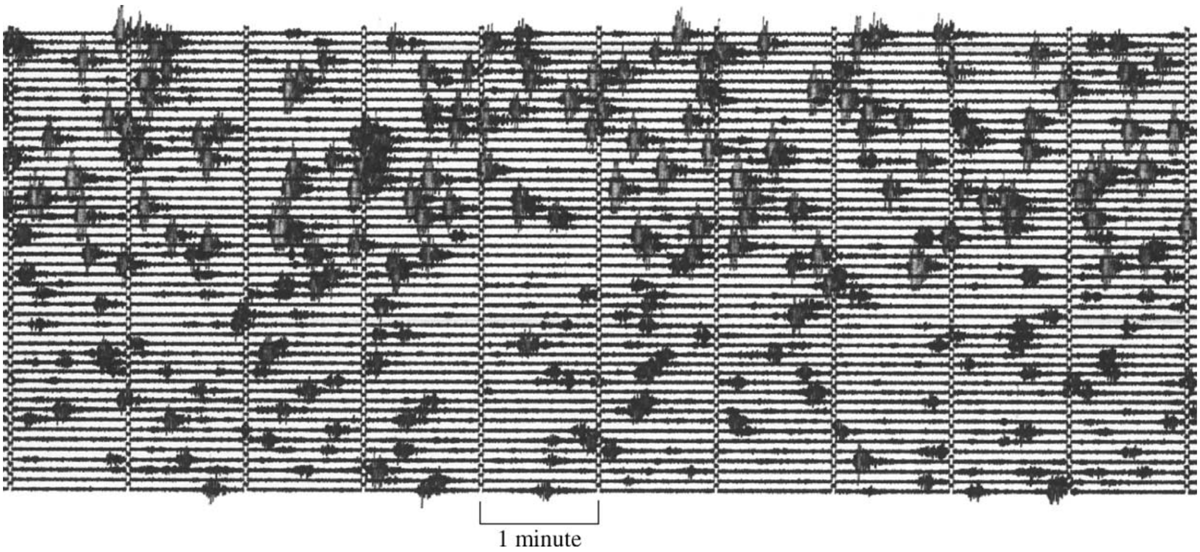

Fig. 2. Section of helicorder record showing 8 hours of data recorded at station SSLN on November 21, 2002. Tick marks represent 1-min intervals. A long-period event occurs every 1–2 min. Event amplitudes decrease in the middle of the section, but the number of events remains high. A detailed count of all events in the 8-h section with signal-to-noise ratio ≥2 results in 160 events before and 138 after the decrease in amplitudes.

In this paper, we present an overview of the seismicity at Shishaldin with a focus on LP earthquakes. We chose to end the time period of this study before the nature of seismicity changed in May 2004. Our purposes are to describe the Shishaldin events in detail, and to document and quantify the main aspects of the events. Shishaldin's unusual behavior makes it difficult to forecast eruptive activity and evaluate volcanic hazards. While other volcanoes monitored by AVO would be likely categorized into an elevated eruption alert level if they had such high rates, Shishaldin's seismicity is considered to be at background level. The observations made at Shishaldin permit us to place constraints on allowable source models, but the 6-station monitoring network is not adequate to fully model source characteristics. We emphasize instead the unusual nature of Shishaldin's seismicity.

2. Geologic setting

Shishaldin Volcano is one of 5 volcanoes located on Unimak Island, the easternmost of the Aleutian Islands, Alaska (Fig. 1). The 2857 m high stratovolcano with pronounced conical symmetry is primarily composed of basalt and basaltic andesite. The cone is about 16 km in diameter at its base, and snowfields and small glaciers cover two-thirds of it year-round. At almost all times, a volcanic plume is emitted from the ~60 m wide vent that is embedded in a small (about 100 m diameter) summit crater (Fig. 3). The relative contribution of meteoric and magmatic gas is unknown, but blue haze and sulfur smell indicates that magmatic gases, such as SO_2, are at least partly involved in the plume activity. Field observations have shown that the plume emanates from the summit crater in the form of discrete puffs (Fig. 3).

With 29 eruptions reported since 1775 (Miller et al., 1998; Nye et al., 2002), Shishaldin is one of the most active volcanoes in the Aleutian Islands. The eruptions have mostly been of Strombolian type, creating small ash and steam plumes, but 11 Subplinian eruptions in the Holocene have also been identified based on the study of tephra deposits (Beget et al., 1998). Shishaldin last erupted in April–May 1999, exhibiting both Strombolian and Subplinian behavior with a plume that reached heights up to 16 km (Nye et al., 2002) and produced 43 million cubic meters of tephra (Stelling et al., 2002).

3. Limited visual and satellite observations

Visual observations of Shishaldin's volcanic activity are limited by its remote setting. Shishaldin is located 1098 km southwest of the AVO office in Anchorage, Alaska, making field observations conducted by AVO relatively rare. Shishaldin is not visible from the nearest population center, False Pass, located ~60 km to the east, although the summit is visible from Cold Bay, a community located ~92 km to the ENE. Occasionally local pilots provide AVO with reports about the ongoing plume activity. Visual observations are further limited by the poor

a)
b)

Fig. 3. (a) A volcanic plume is typically emitted as discrete puffs of gas from the summit crater of the 2857 m high stratovolcano Shishaldin. Photo shows the upper 500 m of the volcano. (b) Shishaldin's summit crater, ~100 m in diameter. The crater walls steeply slope towards the ~60 m wide vent. Isanotski and Round Top volcanoes are visible in the background. View from the west. Photos taken by Tanja Petersen, July 2003.

weather conditions, typical for the Aleutian Islands. Therefore, AVO relies heavily on telemetered data, in particular seismic and satellite data, for monitoring the volcano.

Between September 2000 and April 2004, the only thermal anomalies observed in satellite imagery occurred in 2 days in January 2004 and in 1 day in April 2004 (J. Dehn, written communication, 2004). This rare observation may or may not be due to the geometry of Shishaldin's crater. The steep slopes of the crater (Fig. 3) shield part of the volcano from satellites; hence the satellite has to be more or less directly above the volcano in order to detect heat sources within the deeper parts of the conduit system. Dense meteorological clouds and the volcanic plume itself also frequently limit the satellite imagery.

Interferometric synthetic aperture radar (InSAR) imaging corresponding to the 1999 eruption shows no significant deformation at Shishaldin (Lu et al., 2003). This might be due to the steep, snow and ice covered summit area, which does not maintain coherence. A deformation source at shallow depth right beneath the summit would produce more localized deformation on the upper flanks of the volcano and therefore would be undetectable (Mann, 2002). Other possible scenarios are that any inflation was balanced by successive deflation or simply that no significant deformation took place (Lu et al., 2003). Data from October 2000 to July 2001 show a ~3 cm shallow inflation slightly northwest of Shishaldin's cone (Mann, 2002). However, Mann (2002) further notes that subtle signals such as the one fringe of inflation seen in the Shishaldin interferogram may be due to atmospheric effects rather than deformation of the volcano. Available images were not sufficient to verify the inflation.

The remote setting of Shishaldin volcano allows no definitive information on fluctuations in the strength of the omnipresent summit plume and its possible correlation with the intensity of the seismic activity.

4. Seismic network

In summer 1997, AVO installed a network of six short-period seismic stations around Shishaldin at distances of 5.3–19 km from the vent (Fig. 1). Five of the stations are vertical, short-period L-4C instruments with 1 Hz natural frequency. Station SSLS is a three-component L-22 instrument with a natural frequency of 2 Hz. In July 2003, station SSLN was supplemented with a Chaparral Model 2 microphone. The pressure sensor has a flat response from 0.1 to 200 Hz. The data from all instruments are telemetered to AVO in Fairbanks, where they are displayed as helicorder records on drum recorders and also digitized at a sampling rate of 100 samples/s using a 12-bit digitizer.

Station ISNN suffers from a poor telemetry link, which makes it unreliable especially in the winter months. Stations BRPK and ISTK are located too far from Shishaldin's vent to exhibit reasonable signal-to-noise ratios for small signals; hence they rarely show clear arrivals for LP events. Station SSLN retains the best signal-to-noise ratio when weather conditions are poor, although until July 2003 the data clipped at low amplitude. The clipping, caused by a dysfunction in the recording system, modified the information on frequency content and restricted magnitude estimates. However, on quiet days with relatively high signal-to-noise ratios 5 P-wave first arrival time picks are available for locating larger LP earthquakes; 4 picks are more common. Because LP events commonly lack clear S-waves, P-wave arrivals are the only phases available for the vast majority of events. Even though there are some limitations of the network, the seismic data recorded at Shishaldin provide a high number of clear signals, which can be selected for additional analyses.

5. Classification of event types

The vast majority of Shishaldin's earthquake types can be classified by using schemes similar to the ones developed by Chouet et al. (1994) and Lahr et al. (1994). This classification is based on more general ideas about the physical processes associated with the seismic source. The literature presents a much greater variety of distinct source mechanisms for each event type. However, the earthquake types most commonly observed in volcanic regions include volcanic tremor, volcano-tectonic events, long-period events and hybrids. Event types observed at Shishaldin are described below.

Volcano-tectonic (VT) events are high-frequency earthquakes representing the brittle failure of rocks due to stress changes in volcanic regions. VT events represent a purely elastic source and show characteristics similar to common double-couple tectonic earthquakes located in non-volcanic regimes. They have clear P- and S phases with peak frequencies above 5 Hz and a variety of first motions (Lahr et al., 1994). VT earthquakes occur within or near the volcanic edifice and may or may not be associated with magmatic activity. In March 1999, a shallow (about 1 km below the surface) M_L 5.2 strike-slip earthquake occurred 16 km to the west of Shishaldin (Fig. 1), followed by a several months long aftershock sequence (Moran et al., 2002). Since then the few VT events detected are almost exclusively restricted to the area 10–15 km west of the summit. Another VT cluster is located southeast of the adjacent volcano Isanotski near Cape Lazaref (Fig. 1). An exception to this steady-state behavior was a small swarm of VT events at shallow depths beneath the summit region on 6–7 February 2000.

Long-period events (LP) produce discrete low-frequency seismic signals and are commonly associated with gas and liquid phases within the volcanic conduit (Lahr et al., 1994). They are characterized by emergent onsets due to a gradual increase of fluid-driven oscillation (Lahr et al., 1994). The waveforms are monochromatic with extended codas lasting several tens of seconds. The S-waves of LP events are not distinct. A possible reason for this is that LP events represent a volumetric source that has less excitation of S-waves than an earthquake generated by shear faulting. Short arrival time differences between P, S and surface waves and a finite duration of the source time function enhance the lack of distinct S-waves. At Shishaldin, the vast majority of earthquakes are discrete low-frequency signals with a fairly narrow frequency band between

0.8 and 4 Hz and dominant spectral amplitudes between 1 and 2 Hz (Fig. 4a). These LP events occur at intervals of about 0.5–5 min.

The timing between consecutive puffs in the omnipresent summit plume has been measured with precision over a time period of 20 min based on visual observations from station SSLS on July 13, 2003. It ranges between 15 and 100 s. The LP events recorded during the observation time occur at a similar rate. These short time intervals make it impossible to assign a puff to a specific seismic signal without ambiguity, mainly because the delay between the formation of a

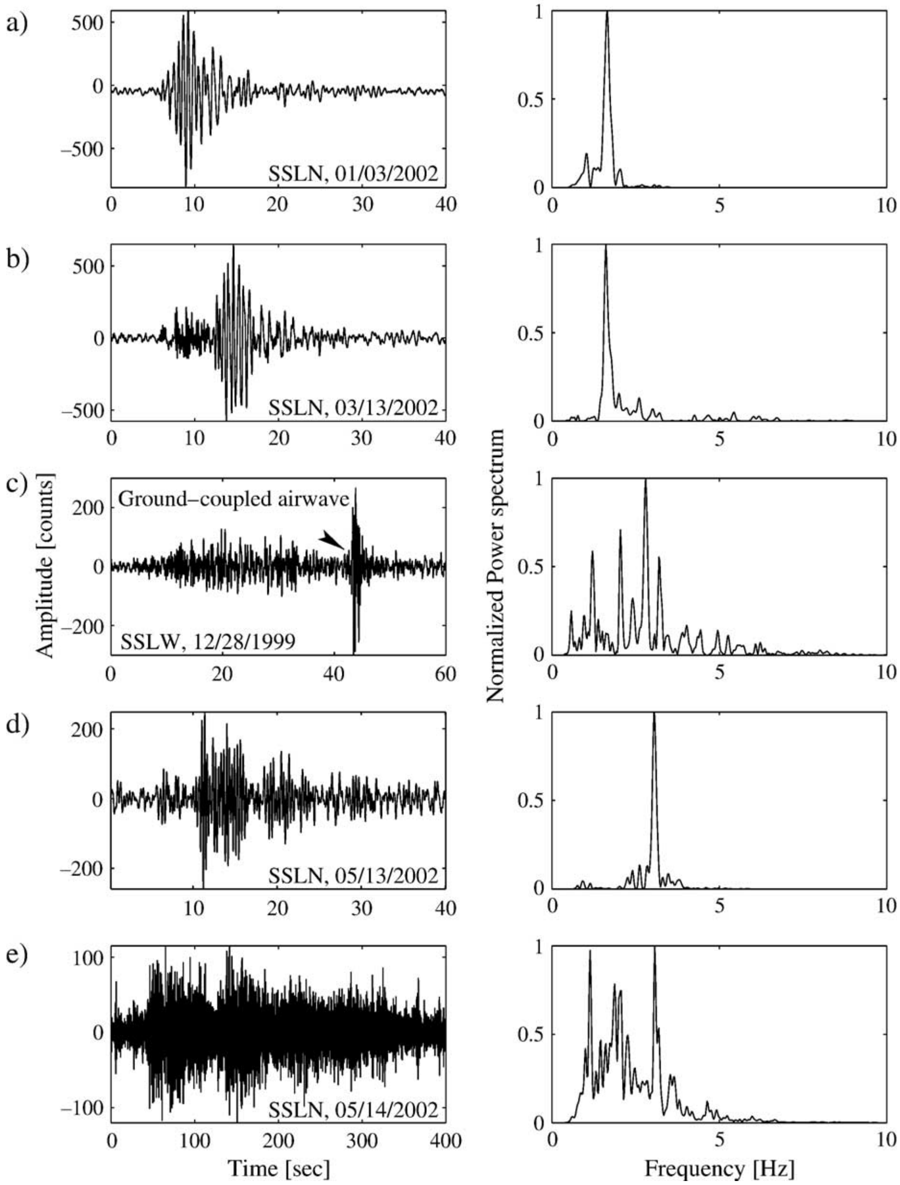

Fig. 4. Seismograms and normalized power spectra for earthquake types commonly seen at Shishaldin. Each spectrum is obtained from a window enclosing the signal. (a) LP event recorded at station SSLN. LP events belong to the most common type of earthquakes seen at Shishaldin. The spectrum exhibits a dominant spectral peak at 1.6 Hz. (b) Coupled event recorded at station SSLN. Note that the low-frequency part of the waveforms is similar to event (a). The preceding higher frequency (4–7 Hz) portion is the distinctive characteristic for the coupled events observed at Shishaldin. (c) Explosion event recorded on station SSLW at 10.1 km from the summit. The airwave also arrived at station SSLS and SSLN, but there the acoustic signal coupled less strongly into the ground. The initial part of the waveform is low frequency, while the airwave has dominant frequencies between 5 and 7 Hz. (d) DLP event recorded at station SSLN in May 2002. The event exhibits a dominant spectral peak at 3 Hz. (e) Volcanic tremor recorded at station SSLN in May 2002. The tremor burst was recorded across the entire network.

puff and its arrival at the crater rim is likely to vary from event to event. A puff produced by an LP event located deep within the conduit is likely to have a larger delay time than puffs induced by a shallower earthquake. Also a weak seismic event may not produce a plume strong enough to be seen as discrete puff. However, the similarity between time intervals of observed puffs and LP events suggests, together with the ubiquity of the summit plume, that the seismic events at Shishaldin are related to degassing processes.

Explosion events are discrete low-frequency earthquakes with an airwave phase. The airwaves are acoustic waves, propagating through the atmosphere at about 331 m/s and couple back into the ground near the seismometer. The deeper the explosion events occur in the conduit, the larger is the seismic arrival compared to the airwave phase (e.g. Mori et al., 1989). During 1999 and 2000, high-frequency signals identified as ground-coupled airwaves were occasionally observed at Shishaldin (McNutt et al., 2000). McNutt et al. (2000) further document that these explosion events were partly accompanied by weak thermal anomalies. Fig. 4c shows an explosion event recorded at Shishaldin.

Hybrid events typically have an impulsive higher frequency onset followed by a low-frequency coda with the same frequency content as LP events (Neuberg et al., 1998). They commonly exhibit a variety of first motions characteristic for VT events (Lahr et al., 1994). The model most commonly used to explain the different phases involves both shear faulting and resonance of an intersecting fluid-filled crack (Lahr et al., 1994). At Shishaldin, events with a hybrid appearance, termed “coupled events”, dominated the March–November 2002 activity (Caplan-Auerbach and Petersen, 2005). They consist of a short-period (4–7 Hz) phase, followed by a long-period (1–2 Hz) signal of larger amplitude. The waveform of the long-period portion is similar to the LP events described earlier. This similarity suggests that LP events and the LP phase of coupled events share common source processes and have nearby origins. The two portions of the coupled events are both highly repetitive, indicating a stable, non-destructive source process for each part (Caplan-Auerbach and Petersen, 2005). Unlike traditional hybrid events, the time separation between the two parts of the signal is highly variable, from 3 to 15 s, a behavior that has been related to temporal changes in gas content (Caplan-Auerbach and Petersen, 2005). Fig. 4b shows an example of a coupled event.

Volcanic tremor is identified by its continuous signal with a low-frequency spectral content of 0.8–8 Hz, typically peaked at 2–3 Hz (McNutt, 1992). Models for volcanic tremor include the response of fluid-filled conduits to sustained pressure fluctuations (Chouet, 1996; Neuberg et al., 2000) and degassing processes of magma (Chouet, 1985; Ripepe et al., 1996, 2001). Fehler (1983), Havskov et al. (1983) and Malone (1983) consider volcanic tremor to be composed of a sustained sequence of LP events, i.e. tremor and LP events are both generated by similar fluid dynamical processes but with different excitation mechanisms (Almendros et al., 2001). Ripepe and Gordeev (1999) present a model in which tremor is generated by the continuous bursting of small gas bubbles. Julian (1994) proposes that tremor oscillations are excited by a non-linear interaction of a single-phased fluid with the irregular conduit through which it is flowing. Extensive volcanic tremor was observed at Shishaldin in relation with the 1999 eruption, and was discussed by Thompson et al. (2002). The only other time volcanic tremor was observed at Shishaldin was in May 2002 when several tremor bursts lasting 3–5 min accompanied a deep long-period event at Shishaldin (Fig. 4e).

Deep long-period (DLP) events occur at about 10–50 km depth and are characterized by emergent onsets, extended codas and strong spectral peaks between 2 and 4 Hz (Fig. 4f; Power et al., 2002). DLP events have been associated with magma movement, are often highly clustered in time and accompanied by volcanic tremor (Power et al., 2002). Since AVO started monitoring Shishaldin, about 13 DLP events, spread out over much of the eastern half of the island, have been located, 5 of which may have been precursors to the 1999 eruption (Power et al., 2002). In May 2002, a DLP appeared as a M_L 1.8 earthquake at a depth of 47 km with an epicenter some 7 km east of Shishaldin’s summit (Dixon et al., 2003); approximately 150 larger LP events located within the shallow summit region were recorded on the same day.

6. Overview of Shishaldin seismicity

AVO uses several methods for monitoring the level of seismicity at Shishaldin, including the “Earthworm” acquisition system that uses a short-term-average/long-term-average trigger algorithm to detect earthquakes. However, the only counting method that provides a continuous quantitative overview of the seismicity throughout the time period since the eruption is referred to as “pseudohelicorder counts”. In this paper we use pseudohelicorder counts, or simply “counts”, to present the number of events per day with the maximum amplitude exceeding a certain threshold (≥6 mm peak-to-peak) on digitally filtered helicorder records (Fig. 5). The 0.8–5 Hz bandpass filter reduces the influence of seismic noise by removing low frequency surf noise and high frequency wind and rainfall noise. The counts are performed on data recorded by an L-22 seismometer. Since this type of instrument is not optimal for recording low frequencies, the number of Shishaldin events that will meet the counting criteria has already been reduced. The vast majority of the events recorded at Shishaldin have very small amplitudes, thus a large number of events fall below the counting criteria. Fig. 6 presents the systematic overview of Shishaldin seismicity provided by pseudohelicorder counts.

During the first year of network operation, from 1997 to 1998, Shishaldin was seismically relatively quiet, except for a few brief swarms of small LP events and a few deep long-period (DLP) events (Power et al., 2002). In early 1999, the counts became more complex (Fig. 6): tremor episodes preceding and accompanying the eruption in April–May 1999 and an M_L 5.2 strike-slip earthquake on March 4 and its aftershock sequence dominated the seismic data through May 1999. After the eruption, seismicity was low through early September. Then it increased again in September 1999, composed exclusively of LP and explosion events. Since that time, the background seismicity has remained high but variable. An episode

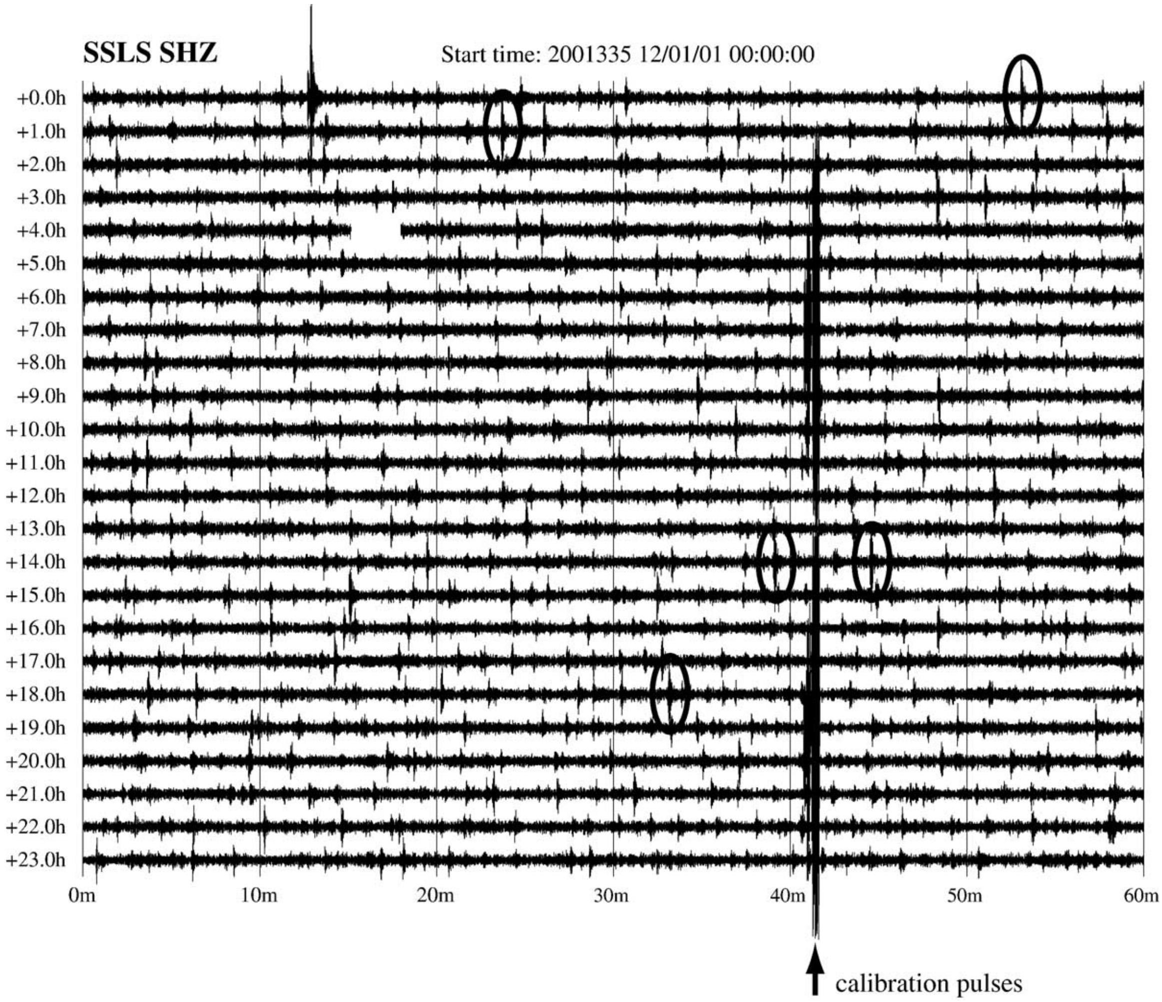

Fig. 5. Example of pseudohelicorder plot showing 24 h of continuous data (December 3, 2001; station SSLS, vertical component). The data have been bandpass filtered between 0.8 and 5 Hz to reduce noise. In order to be included in the pseudohelicorder counts, the event has to be a local earthquake and the maximum amplitude has to contact the two adjacent lines. The threshold value is equivalent to local magnitude 1.1. Earthquakes are considered as being local if the P- and S-wave arrivals are not clearly distinguishable from each other on the pseudohelicorder plots; ambiguous events are resolved using helicorder records, which have higher temporal resolution. Ovals mark the 5 events included in the pseudohelicorder counts for that day.

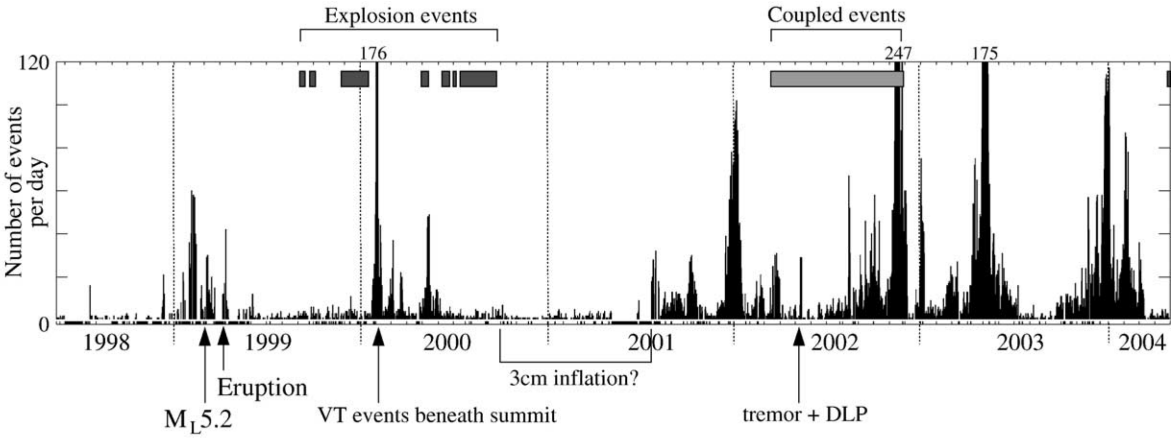

Fig. 6. Filtered digital ("pseudohelicorder") daily counts for Shishaldin plotted from May 1998 through April 2004. The interval between two tick marks on the time axis (top) represents 1 month. The vertical bars show the number of events per day included in the counts. Negative values indicate days for which no counts are available due to wind noise. The horizontal bars at the top mark periods during which "explosion events" and "coupled events" occurred (see text). The M_L 5.2 earthquake in March 1999 and Shishaldin's most recent eruption in April–May 1999 are labeled. A small swarm of VT events at shallow depths beneath the summit region occurred February 6–7, 2000 (2 days after 176 events were included in the counts). InSAR data from October 2000 to July 2001 show a potential ~3 cm shallow inflation at the northwest flank of Shishaldin. Tremor bursts and a DLP event were recorded in May 2002.

of very high counts with up to 176 counted events per day occurred in February 2000. A small swarm of VT events beneath the summit was observed for two days at the beginning of this episode. Since July 2001 the average number of counts per day has increased resulting in a mean value greater by a factor of 3. Four episodes of very high counts have been observed since then. During these episodes, 6–10 months apart, the counts remained very high for several weeks reaching up to 247 counted events per day. Overall, since 1999, Shishaldin seismic activity has had a rate that is almost 3 orders of magnitude higher than that seen at other volcanoes monitored by AVO and at Shishaldin during 1997–1998. Pseudohelicorder counts for Akutan Volcano, one of the most active volcanoes in the Aleutian arc, for example, show about one event per week. The counts for Shishaldin vary between 1 (occasionally 0, but only for up to a couple of days at a time) and 247 events per day. It must be noted that these values reflect only the larger events; there are always several hundreds to about 1500 smaller events every day that do not meet the selection criteria.

7. Estimation of magnitudes and energy

In order to relate the seismicity observed at Shishaldin to other volcanic regions, earthquake counts have to be further quantified. The first step is to determine the magnitudes of counted events. We can then estimate the amount of energy released per day.

The determination of magnitudes for LP events is not easy because the location of most of these events is not always possible. Furthermore, the source mechanisms for earthquakes generated by fluid processes are still poorly understood, hence the local magnitude scale, M_L, developed for tectonic earthquakes by Richter (1935), may not be appropriate for LP events. However, because at present there is no known way to quantify the size of LP events more accurately, the magnitudes for the thousands of located LP events at Shishaldin are local Richter magnitudes computed by HYPOELLIPSE (Lahr, 1999) using a measure of peak amplitude. These magnitudes vary between 0.4 and 1.8. Assuming that the unlocated LP events also originate in the summit region we can provide estimates of the magnitudes of these events. The similarity in waveforms between located and unlocated events supports this assumption. The located events provide a reasonable reference for scaling pseudohelicorder and helicorder records. The vast majority of LP events have magnitudes <1.0. The amplitude threshold value for the pseudohelicorder counts is equivalent to $M=1.1$, hence a significant number of events are not included in the counts.

The energy, E, of the seismic source can be estimated using an empirical formula for local earthquakes, $\log E = 9.9 + 1.9M_L - 0.024M_L^2$ (Gutenberg and Richter, 1956), where M_L is the local magnitude. This magnitude scale may not be reasonable for LP events and does not provide absolute values, but can be used as a consistent mean of looking at energy release over time. The number of events per day and their magnitudes are needed to approximate the amount of energy released per day. In order to extrapolate pseudohelicorder counts to the overall number of earthquakes per day, "detailed counts" have been accomplished for a few days with very low wind noise. Detailed counts are performed on helicorder records, including all events with a signal-to-noise ratio of ≥ 2. The amplitudes are measured by hand; hence this method is very time consuming and has only been done for a few selected days. The smallest events included in the detailed counts have an estimated magnitude of $M_L = 0.03$. The total number of events per day counted for the 7 selected days varies from 349 to 1505 (Fig. 7). The counted events had magnitudes as large as $M_L = 1.2$. The seismic energy released per day, calculated from the detailed counts, ranges from 1.86×10^{13} to 5.75×10^{14} ergs, which is equivalent to one $M_L = 1.8$–2.6 earthquake. The relation between the number of larger ($M \geq 1.1$) events and smaller ($M < 1.1$) events is not consistent. The ratio of small-to-larger events varies by a factor between 3 and 185; hence we are unable to extrapolate total daily energy release from the pseudohelicorder counts. The observed variation in the relative abundance of small events compared to larger ones itself needs further investigation and shall be addressed in future studies.

8. Repeating LP events at Shishaldin

Visual inspection of seismic records exposed repetitive LP events with extremely similar waveforms. We use a technique based on waveform cross-correlation (Caplan-Auerbach and Petersen, 2005) to identify and extract repeating events. In this method a "reference event", a section of an event with a good signal-to-noise ratio, is cross-correlated with segments of the continuous data. The selected reference event is 8 seconds long, which is an appropriate duration of the strong part of the signal (Fig. 4a). The time at which two signals show the maximum cross-correlation value defines the beginning of a data segment. The spectral-coherence between the reference event and each data segment is calculated and averaged over a frequency band between 0.5 and 4 Hz. Events with a mean coherence exceeding a threshold of 0.9 are extracted and aligned in time series. We chose to use the coherence as a measure of how well two signals correlate rather than using correlation coefficients because the monochromatic nature of LP waveforms often causes misalignment by an integer number of wavelengths. Fig. 8 shows events exceeding a minimum spectral coherence of 0.9, which were extracted as "repeating events", i.e., events with highly similar waveforms. The waveform similarity is also seen at other stations; hence

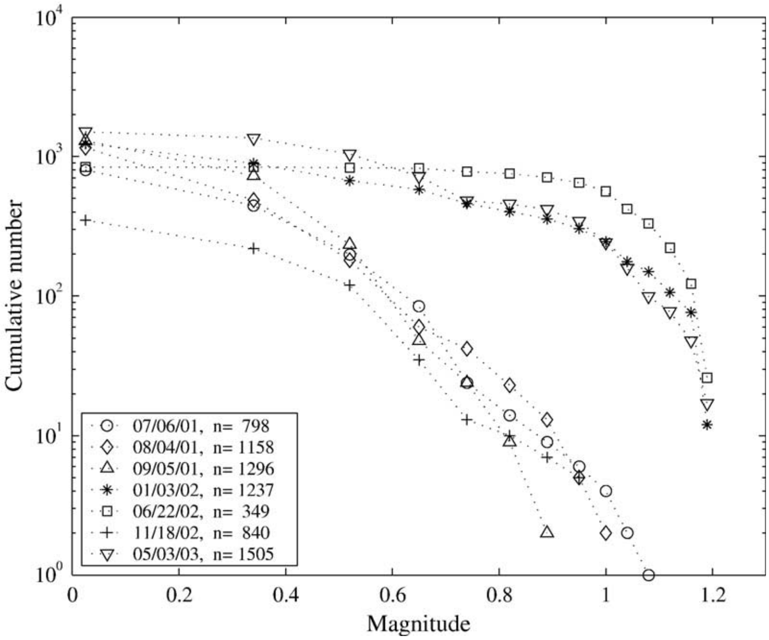

Fig. 7. Detailed helicorder counts for 7 different days plotted as frequency-magnitude distributions. The "estimated magnitude" for unlocatable low-frequency events has been calculated relative to located events using Richter's local magnitude scale and assuming that all low-frequency events originate in the summit region. The total number of events per day (n) is listed in the legend. Note that when the number of large events increases, the number of small events does not change significantly.

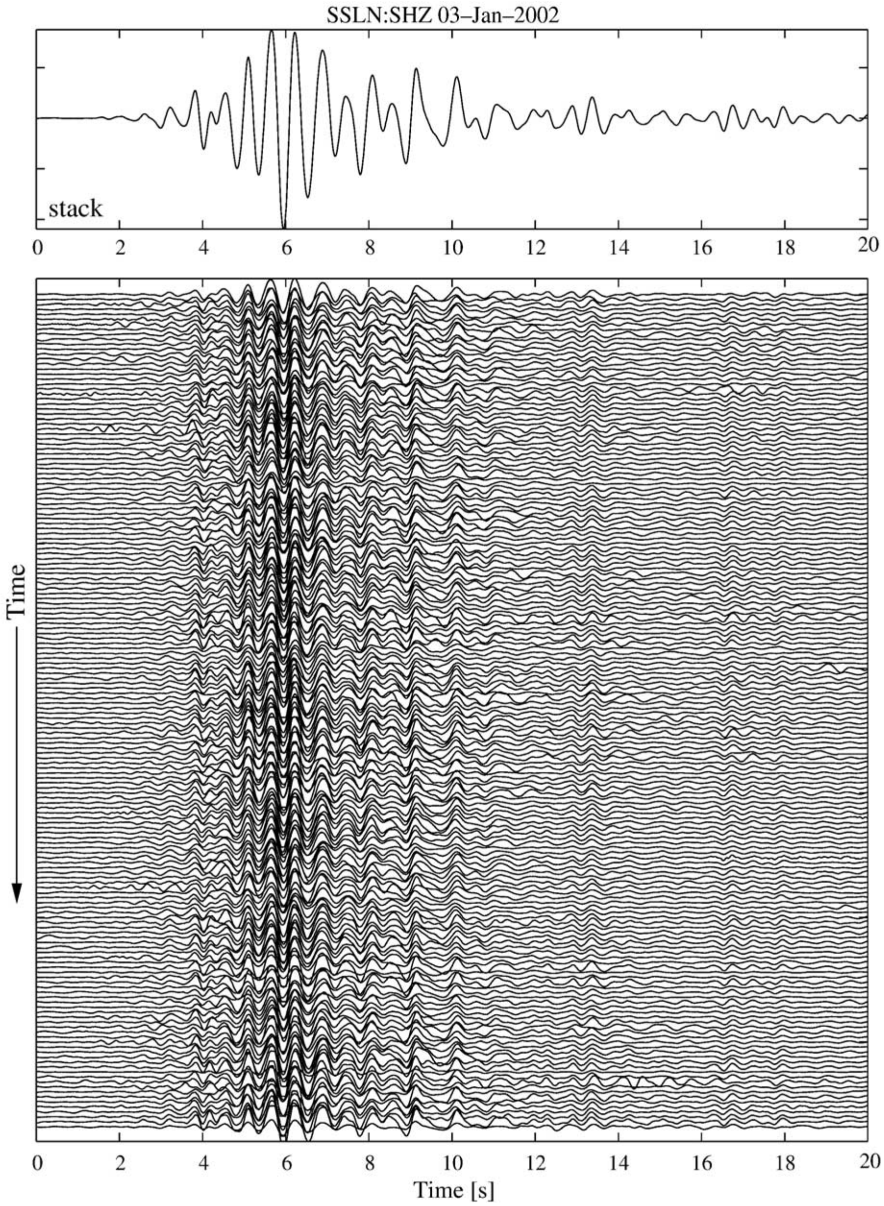

Fig. 8. Examples of repeating events at Shishaldin. LP events recorded at station SSLN on January 3, 2002. The cluster was extracted by cross-correlation. The spectral-coherence values for these events are ≥ 0.9. The upper part of the plot shows a stack of all events in the lower part. The waveform similarity between the events is also seen on other stations.

the similarity is due to source rather than path or site effects. In order to produce similar waveforms at a seismic station the source locations of the individual events can only vary within ~500 m (1/4 of the approximated dominant wavelength; e.g., Geller and Mueller, 1980). The source process has to be stable and non-destructive in order to act repeatedly. At any given time there is generally only one major family of repeating events, dominating Shishaldin's seismic activity for several days up to several months (Caplan-Auerbach and Petersen, 2005). These different repeating events exhibit subtle differences in event waveforms and power spectra (Fig. 9).

9. Locations

Determining the locations of LP events using traditional arrival time methods is usually difficult or impossible because of their emergent onsets and the lack of clear S-waves. At Shishaldin, the large distance (5.3–

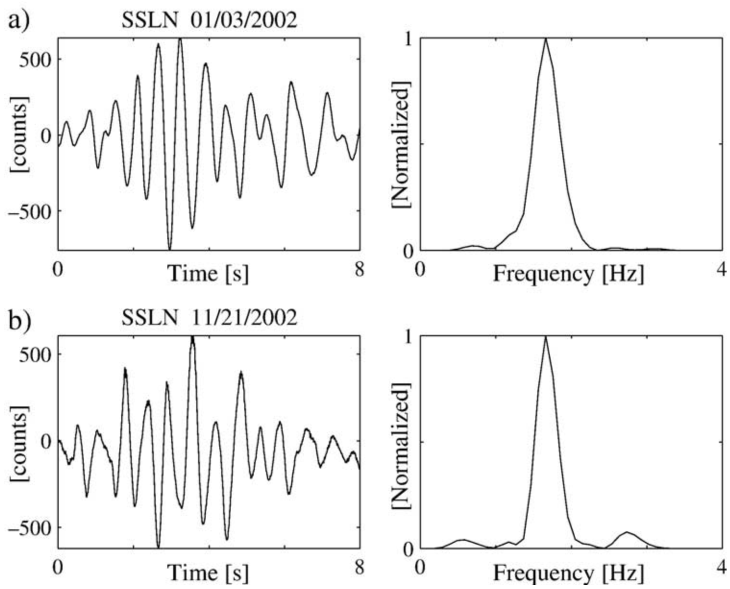

Fig. 9. Waveforms and normalized power spectra of reference events recorded at station SSLN on (a) 3 January 2002 and (b) 21 November 2002. The spectral-coherence between the two reference events is 0.66. Each reference event represents a family of repeating events.

19 km) between the source region and the local seismic network, and the small size of the events, results in a low signal-to-noise ratio for the majority of events. Because it is already difficult to locate LP events due to their emergent onsets, small amplitudes make it even more difficult to identify or define the P-wave arrivals precisely. Furthermore, the noise levels on network stations due to wind and telemetry problems sometimes leave only a few readings available for earthquake locations. Therefore, at Shishaldin only a small percentage (<10%) of the events that triggered the Earthworm data acquisition system are locatable (Dixon et al., 2003). The velocity structure around Shishaldin is poorly constrained. The velocity model used by AVO was originally constructed for Pavlof volcano (McNutt and Jacob, 1986), located 160 km to the ENE of Shishaldin. Shishaldin's seismic stations span a ~400 m difference in elevation. These factors, together with the lack of S-waves and the difficulties of picking P-wave arrivals with accuracy, combine to produce a severely limited depth resolution. Although precise hypocentral locations are not available for the LP events, preliminary locations obtained by using HYPOELLIPSE (Lahr, 1999) indicate that they are located beneath the summit at shallow (0–3 km) depths (Fig. 10) (Dixon et al., 2002, 2003, 2004). We only selected events with HYPOELLIPSE quality factors A and B, indicating 68% confidence levels for horizontal and vertical location errors of <2.67 km (Lahr, 1999). These shallow locations are supported by acoustic data recorded by the pressure sensor (Petersen et al., 2004). Nearly every seismic event is accompanied by an infrasonic signal; which suggests that the source is located within the conduit system at very shallow depths.

In order to improve signal-to-noise ratios and thus to allow more precise arrival time picks, repeating events were aligned by cross-correlation and stacked at each station. The stacked events were located using HYPOELLIPSE. The location places a cluster of repeating events (recorded on 3 January 2002) about 1 km west of the summit at shallow depth (~2 km below summit). Although standard errors calculated by HYPOELLIPSE indicate that these hypocentral depths are well constrained, uncertainties in the velocity model and the lack of S-waves suggest that in fact there is a large degree of uncertainty in earthquake depth. A second cluster of repeating events (recorded on 21 November 2003) is located directly beneath the summit. The depth for this cluster is poorly resolved. The epicentral locations for the two clusters are shown in Fig. 10. The locations of these two clusters confirm that the bulk of LP events most likely originate beneath Shishaldin's summit area.

Although hypocentral depths at Shishaldin are poorly constrained using standard location algorithms, other techniques may be used to confirm that a shallow depth is reasonable. For events with associated airwaves, depths can be constrained by using the difference in arrival time between the P-wave and airwave. We selected a representative explosion event with a good

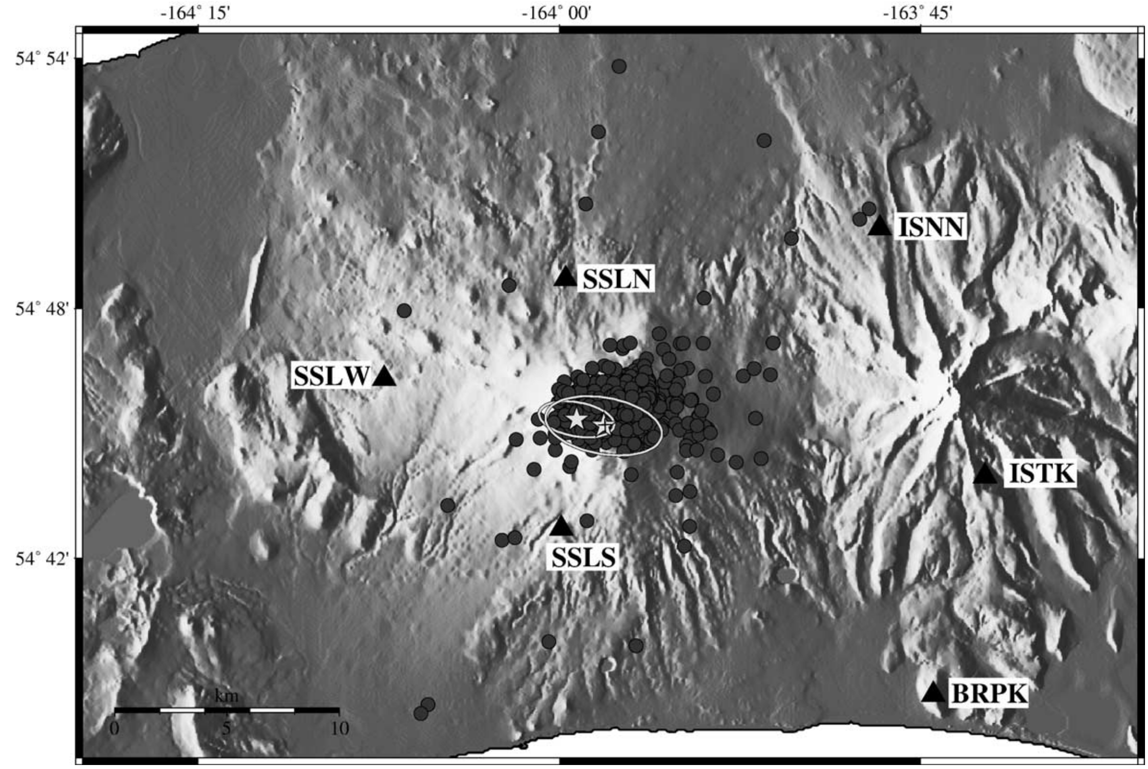

Fig. 10. Epicenters for LP and coupled events at Shishaldin since 1997 (Dixon et al., 2002, 2003, 2004), located with 68% confidence levels for horizontal and vertical locations of <2.67 km (Lahr, 1999). The vast majority originate beneath Shishaldin's summit (black cross) at depths of 0–3 km. Magnitudes vary between 0.4 and 1.8. Epicentral locations (star) and error ellipsoids (68% confidence) for stacked repeating events from 3 January 2002 and 20 November 2002 are marked.

signal-to-noise ratio recorded at station SSLN and SSLW on 30 April 2004 (18:20:10 UTC), and picked arrival times with a 0.1 s uncertainty for SSLW and 0.2 s for SSLN. For station SSLW (9.8 km horizontal and 2.2 km vertical distance from summit), the arrival time difference (Δt) is 26.1 s (Fig. 11). The arrival time

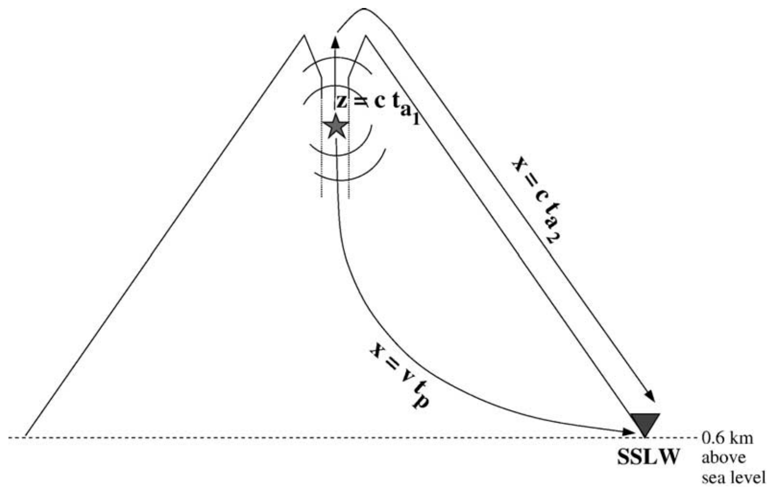

Fig. 11. Illustration of how the depth of explosion events can be estimated by using the time difference ($\Delta t = 26.1$ s) between P-wave arrival (t_p) and airwave arrival ($t_a = t_{a1} + t_{a2}$) measured for an earthquake with a ground-coupled airwave phase recorded at station SSLW at a distance of $x = 10.1$ km from the summit. Assuming an acoustic velocity (c) of 0.331 km/s and a seismic velocity (v) of 2.0 km/s, the source is located at a depth (z) of about 0.2 km.

difference for station SSLN (6.3 km horizontal and 2.1 km vertical distance from summit) is 17.2 s. We assume the simplest model for which the airwave from the summit to the seismic station and the seismic wave are assumed to travel the same distance (Hagerty et al., 2000). This assumption is reasonable for cases in which the station-summit distance is much greater than the depth (z) (Hagerty et al., 2000). The depth $z = c(\Delta t - [1/c - 1/v]x)$ of the source can be estimated by using reasonable values for the acoustic velocity (c) and the seismic velocity (v). Assuming an acoustic velocity of 0.331 km/s (speed of sound through air at 0 °C) and a seismic velocity of 3.05 km/s (P-wave velocity for upper 3 km of Pavlof volcano; McNutt and Jacob, 1986), the source would be spuriously located outside the volcano. A value of $v = 2.0$ km/s results in a depth of about 0.2 km. Although we note that these values are only approximate, the calculations confirm that the source is likely located at very shallow depth.

10. Constraints on allowable source models

There are two general trends for models explaining the generation of LP events related to the presence of gas within fluid bodies; one is based on bubble coalescence and the other on conduit oscillation induced directly by fluid transfer. The sudden coalescence of gas bubbles, accumulating below a structural barrier, into a single gas bubble has been studied in laboratory experiments (Jaupart and Vergniolle, 1988, 1989) and has been used to explain the source of low-frequency events at Stromboli volcano (Ripepe and Gordeev, 1999). The other trend of models is based on pressure fluctuations promoting crack or conduit oscillation induced by fluid transfer through a magmatic or hydrothermal conduit system (e.g. Chouet et al., 1994; Chouet, 1996). A similar fluid dynamic process is used to explain seismic tremor but with a different excitation mechanism producing a sustained signal rather than the discrete signal observed for LP events (Chouet, 1996). Hellweg (2000) considers turbulent flow conditions as the generator for conduit oscillation. Hellweg (2000) describes how eddies are able to develop on the downstream side of an object and that they produce density variations that propagate through the conduit system as sound and seismic waves. An alternate consideration is presented by Zimanowski (1998) who suggests that a phreatomagmatic explosion caused by a near surface interaction between groundwater and magmatic melt may trigger a seismic low-frequency event. A phreatic explosion resulting from the pressurization of a hydrothermal system may have the same effect.

Possible constraints on trigger mechanisms for LP events observed at Shishaldin include that the process must be capable of producing at least one LP event every 0.5–5 min. The system generates almost exclusively discrete seismic events instead of releasing energy in the form of tremor. The latter was dominant during the 1999 eruption, but has been rarely observed since late 1999. The trigger mechanism must be capable of generating events that exhibit varying amplitudes, at a relatively constant rate. The similarity of waveforms within certain clusters of repeating events requires a source mechanism stationary within only a few hundreds of meters (1/4 of a wavelength); the source is acting repeatedly and, therefore, is non-destructive. The lack of VT events indicates that the conduit represents an open system through which gas can constantly escape without causing brittle failure of surrounding volcanic rocks. The system produced a puffing volcanic plume, even during 1997 and 1998 (P. Stelling, personal communication, 2004) when Shishaldin was seismicially quiet.

All of the source models described in the above paragraph may satisfy these criteria. The last condition is the most complex one, because it requires an explanation of how the system changed from gas release without major seismic activity to gas release accompanied by LP events. A possible scenario may be that during 1997 and 1998 the volcanic system was degassing in the form of free gas bubble nucleation, also called a “soda bottle” system and described by Ripepe and Gordeev (1999) and Hellweg (2000). The amount of gas released from the magma through the conduit may have been too small to form seismic signals large enough to be recorded. During the 1999 eruption the conduit system may have been modified. Since then the gas released from the magma column at greater depths in the volcanic system, has to pass obstacles in the conduit such as fallback deposits. In late 1999 the system recovered from the eruption and pressurized again. The velocity of the gas flow increased within the narrowed conduit and past the obstacle produces turbulent flow features, similar to the eddies described by Hellweg (2000). However, these are assumptions solely based on the criteria for possible source models described above; the underlying processes causing Shishaldin’s LP events are still poorly understood and remain a matter of future work. A denser seismic network is needed to get more precise locations in order to better constrain allowable source models.

11. Discussion and conclusions

The continuous high level of LP seismicity beneath Shishaldin's summit has only been observed starting in late 1999, which suggests that the 1999 eruption itself and/or the associated M_L 5.2 earthquake changed the nature of the conduit system and started a new regime of seismic activity at Shishaldin. The overall increase in seismicity since July 2001 may indicate another regime. The potential ~3 cm shallow inflation northwest of the cone based on InSAR data described by Mann (2002) occurred sometime between October 2000 and July 2001. The inflation is unconfirmed due to the lack of additional data, but assuming the InSAR signal truly results from the volcano, the inflation may have preceded the change in seismic activity. Magma accumulation is a likely source for inflation. However, since late 1999, the nature of seismic activity has changed through time via the evolution of systematic differences in event waveforms (Petersen et al., 2002). Time periods of a few days to several months during which repeating LP events occur have been observed. The event appearance varying between different temporal clusters of repeating events probably reflects subtle differences in locations and processes. The event sizes vary over time, but the rates remain roughly constant. The processes causing the variation in event sizes may be related to changes in gas and/or heat flux. The LP source is located within the conduit system; the source processes involving fluid and gas are still poorly understood. However, the conduit system is capable of releasing a large amount of seismic energy without significant stress changes or explosive eruptions. As indicated by the lack of VT events, it represents an open system allowing the release of gas and energy without the opening of new cracks. The level of degassing seems to vary somewhat but is steady enough to produce the almost continuous high background level of LP events observed at Shishaldin. Because the system is open, the high level of seismicity may not indicate a hazardous state. Persistent tremor combined with thermal anomalies in the satellite imagery would indicate rapid degassing with an increased gas flux and a heat source that has moved to shallow parts of the volcano. In any case, sealing of the conduit leading to an extreme increase in gas pressure would be a major concern. Therefore, a change in seismicity such as a conversion from LP to VT seismicity, suggesting a sealed system or the occurrence of volcanic tremor together with thermal anomalies would raise the alert level for a possible eruption. In fact, in May 2004, AVO went from Level of Concern Color Code green to yellow for Shishaldin, because of continuous tremor and thermal anomalies observed in the satellite data.

Shishaldin is unusual among volcanoes in its long-lasting high level of LP seismicity without preceding or accompanying eruptive activity. For example, at Popocatepetl Volcano, a high rate of LP seismicity lasted from 1994 to 2000 (Arciniega-Ceballos et al., 2003), but it accompanied eruptive activity including explosions with ash plume heights of up to 12 km and lava dome growth. At Unzen Volcano, a maximum of ~110 summit earthquakes ($M \geq 0$) per day were observed during the initial phase of the vigorous endogenous growth of the lava dome (November 1993–January 1994) (Nakada et al., 1999). A swarm of more than 4000 LP events directly preceded the 1989–1990 eruption of Redoubt Volcano, but only lasted for 23 h (Power et al., 1994; Benoit and McNutt, 1996). Benoit and McNutt (1996) studied 136 earthquake swarm durations that are not associated with eruptive activity. The mean duration for these swarms is 3.5 days and only 3 of these swarms had durations exceeding 1 year: Rabaul exhibited a swarm of shallow VT earthquakes that lasted 630 days and was accompanied by a caldera floor uplift of 10 cm/year; at Adagdak, a swarm of VT events located at ~5 km depth lasted 865 days; and at Long-Valley, a migrating swarm of VT events lasted 570 days (Benoit and McNutt, 1996). Usu Volcano presented a swarm of similar duration as Shishaldin. The swarm lasted 4 years and 7 months, but Usu's strongest activity accompanied the eruption and included mostly VT earthquakes (Okada et al., 1981; Benoit and McNutt, 1996). On Montserrat, LP events usually occur in swarms starting at a rate of about one event every 1–2 min, but the events occasionally merge into tremor and the swarms last only for a few hours to several days (Neuberg et al., 2000). Thus, the conjunction between a high rate of LP seismicity, extended swarm duration, lack of VT events beneath the summit area and absence of volcanic tremor and eruptive activity is a rarely observed occurrence. This behavior at Shishaldin stands out from many other volcanoes anywhere in the world.

Acknowledgements

We thank our colleagues at the Alaska Volcano Observatory for helpful comments regarding Shishaldin seismicity. We are especially grateful to AVO analyst Scott Stihler for locating Shishaldin earthquakes and to Guy Tytgat for installing and maintaining the Shishaldin monitoring network. We also thank Dave Hill and Randy White of the U.S.G.S. for helpful suggestions that improved the manuscript. Hiroyuki Kumagai and an anonymous reviewer provided thorough and valuable reviews. Several figures were produced using the Generic Mapping Tools software by Wessel and Smith (1998).

References

Almendros, J., Chouet, B., Dawson, P., 2001. Spatial extent of a hydrothermal system at Kilauea Volcano, Hawaii, determined from array analyses of shallow long-period seismicity: 2. Results. J. Geophys. Res. 106 (7), 13581–13597.

Arciniega-Ceballos, A., Chouet, B., Dawson, P., 2003. Long-period events and tremor at Popocatepetl volcano (1994–2000) and their broadband characteristics. Bull. Volcanol. 65, 124–135.

Beget, J., Nye, C., Stelling, P., 1998. Postglacial collapse and regrowth of Shishaldin Volcano, Alaska, requires high eruption rates. EOS Trans. 70, S359.

Benoit, J.P., McNutt, S.R., 1996. Global Volcanic Earthquake Swarm Database 1979–1989. U.S. Geological Survey Open-File Report OF_96-69, p. 334.

Caplan-Auerbach, J., Petersen, T., 2005. Repeating coupled earthquakes at Shishaldin Volcano, Alaska. J. Volcanol. Geotherm. Res. 145, 151–172.

Chouet, B.A., 1985. Excitation of a buried magmatic pipe: a seismic source model for volcanic tremor. J. Geophys. Res. 90, 1881–1893.

Chouet, B.A., 1996. Long-period volcano seismicity: its source and use in eruption forecasting. Nature 380, 309–316.

Chouet, B.A., Page, R.A., Stephens, C.D., Lahr, J.C., Power, J.A., 1994. Precursory swarms of long-period events at Redoubt Volcano (1989–1990), Alaska: their origin and use as a forecasting tool. J. Volcanol. Geotherm. Res. 62, 95–135.

Dixon, J.P., Stihler, S.D., Power, J.A., Tytgat, G., Estes, S., Moran, S.C., Paskievitch, J., McNutt, S.R., 2002. Catalog of earthquake hypocenters at Alaskan volcanoes: January 1, 2000 through December 31, 2001. U.S. Geological Survey Open-File Report OF 02_0342. 56 pp.

Dixon, J.P., Stihler, S.D., Power, J.A., Tytgat, G., Estes, S., Moran, S.C., Paskievitch, J., Sanchez, J.J., McNutt, S.R., 2003. Catalog of earthquake hypocenters at Alaskan volcanoes: January 1, 2002 through December 31, 2002. U.S. Geological Survey Open-File Report OF 03_0267. 58 pp.

Dixon, J.P., Stihler, S.D., Power, J.A., Tytgat, G., Moran, S.C., Sanchez, J.J., McNutt, S.R., Estes, S., Paskievitch, J., 2004. Catalog of earthquake hypocenters at Alaskan volcanoes: January 1 through December 31, 2003. U.S. Geological Survey Open-File Report OF 04_1234. 69 pp.

Fehler, M., 1983. Observations of volcanic tremor at Mount St. Helens Volcano. J. Geophys. Res. 88, 3476–3484.

Geller, R.J., Mueller, C.S., 1980. Four similar earthquakes in central California. Geophys. Res. Lett. 7 (10), 821–824.

Gil Cruz, F., Chouet, B.A., 1997. Long-period events, the most characteristic seismicity accompanying the emplacement and extrusion of a lava dome in Galeras Volcano, Colombia, in 1991. J. Volcanol. Geotherm. Res. 77, 121–158.

Gutenberg, B., Richter, C.F., 1956. Magnitude and energy of earthquakes. Ann. Geofis. 9, 1–15.

Hagerty, M.T., Schwartz, S.Y., Garcés, M.A., Protti, M., 2000. Analysis of seismic and acoustic observations at Arenal Volcano, Costa Rica, 1995–1997. J. Volcanol. Geotherm. Res. 101, 27–65.

Harlow, D.H., Power, J.A., Laguerta, E., Ambubuyog, G., White, R.A., Hoblitt, R.P., 1997. Precursory seismicity and forecasting of the June 15, 1991 eruption of Mount Pinatubo, Philippines. In: Newhall, C., Punongbuyan, R. (Eds.), Fire and Mud. University of Washington Press, pp. 285–304.

Havskov, J., De la Cruz-Reyna, S., Singh, S.K., Medina, F., Gutierrez, C., 1983. Seismic activity related to the March–April, 1982 eruptions of El Chichon Volcano, Chiapas, Mexico. Geophys. Res. Lett. 10, 293–296.

Hellweg, M., 2000. Physical models for the source for Lascar's harmonic tremor. J. Volcanol. Geotherm. Res. 101, 183–198.

Jaupart, C., Vergniolle, S., 1988. Laboratory models of Hawaiian and Strombolian eruptions. Nature 331, 58–60.

Jaupart, C., Vergniolle, S., 1989. The generation and collapse of a foam layer at the roof of a basaltic magma chamber. J. Fluid Mech. 203, 347–380.

Julian, B., 1994. Volcanic tremor: nonlinear excitation by fluid flow. J. Geophys. Res. 99 (6), 11859–11877.

Lahr, J.C., 1999. HYPOELLIPSE: a computer program for determining local earthquake hypocentral parameters, magnitude, and first motion pattern (Y2K compliant version). U.S. Geological Survey Open-file Report OF_99-023. 112 pp.

Lahr, J.C., Chouet, B.A., Stephens, C.D., Power, J.A., Page, R.A., 1994. Earthquake classification, location, and error analysis in a volcanic environment: implications for the magmatic system of the 1989–1990 eruption at Redoubt Volcano, Alaska. J. Volcanol. Geotherm. Res. 62, 137–151.

Lu, Z., Masterlark, T., Wicks Jr., C., Thatcher, W., Dzurisin, D., Power, J., 2003. Interferometric synthetic aperture radar studies of Alaska volcanoes. Earth Obs. Mag. 12 (3), 8–18.

Malone, S.D., 1983. Volcanic earthquakes: examples from Mount St. Helens. In: Kanamori, H., Boshi, E. (Eds.), Earthquakes: Observations, Theory and Interpretation. Elsevier, Amsterdam, pp. 436–455.

Mann, D., 2002. Deformation of Alaskan volcanoes measured using SAR interferometry and GPS. PhD thesis, University of Alaska Fairbanks, August 2002. 122 pp.

McNutt, S.R., 1992. Volcanic Tremor. In: Nierenberg, W.A. (Ed.), Encyclopedia of Earth System Science vol. 4. Academic Press, San Diego, CA, pp. 417–425.

McNutt, S.R., Jacob, K.H., 1986. Determination of large-scale velocity structure of the crust and upper mantle in the vicinity of Pavlof volcano, Alaska. J. Geophys. Res. 91 (5), 5013–5022.

McNutt, S.R., Dehn, J., Gardner, J., 2000. Phreatic explosions at Shishaldin Volcano, Alaska, September 1999 to August 2000. EOS Trans. Am. Geophys. Union 81 (48) (Fall Meet. Suppl., Abstract V22B-12).

Miller, T.P., McGimsey, R.G., Richter, D.H., Riehle, J.R., Nye, C.J., Yount, M.E., Dumoulin, J.A., 1998. Catalog of the historically active volcanoes of Alaska-Shishaldin Volcano. U.S. Geological Survey Open-File Report, 98-482. 104 pp.

Moran, S.C., Stihler, S.D., Power, J.A., 2002. A tectonic earthquake sequence preceding the April–May 1999 eruption of Shishaldin Volcano, Alaska. Bull. Volcanol. 64, 520–524.

Mori, J., Patia, H., McKee, C., Itikarai, I., Lowenstein, P., De Saint Ours, P., Talai, B., 1989. Seismicity associated with eruptive activity at Langila Volcano Papua New Guinea. J. Volcanol. Geotherm. Res. 38, 243–255.

Nakada, S., Shimizu, H., Ohta, K., 1999. Overview of the 1990–1950 eruption at Unzen Volcano. J. Volcanol. Geotherm. Res. 89, 1–22.

Neuberg, J., Baptie, B., Luckett, R., Stewart, R., 1998. Results from the broadband seismic network on Montserrat. Geophys. Res. Lett. 25, 3661–3664.

Neuberg, J., Luckett, R., Baptie, B., Olsen, K., 2000. Models of tremor and low-frequency earthquake swarms on Montserrat. J. Volcanol. Geotherm. Res. 101, 83–104.

Nye, C.J., Keith, T., Eichelberger, J.C., Miller, T.P., McNutt, S.R., Moran, S.C., Schneider, D.J., Dehn, J., Schaefer, J.R., 2002. The 1999 eruptions of Shishaldin Volcano Alaska: monitoring a distant eruption. Bull. Volcanol. 64, 507–519.

Okada, H., Watanabe, H., Yamashita, H., Yokoyama, I., 1981. Seismological significance of the 1977–1978 eruptions and the magma intrusion process of Usu Volcano, Hokkaido. J. Volcanol. Geotherm. Res. 9, 311–334.

Petersen, T., Caplan-Auerbach, J., McNutt, S.R., 2002. Temporal distribution and rates of repetitive low-frequency earthquakes at Shishaldin Volcano, Alaska. EOS Trans. Am. Geophys. Union 83 (47), V21A–V1173. (Fall Meet. Suppl., Abstract).

Petersen, T., Caplan-Auerbach, J., McNutt, S.R., 2004. The Continuously High Level of Long-Period Seismicity at Shishaldin Volcano, Unimak Island, Alaska, 1999 to 2004. Abstract s08d_pf_136, IAVCEI General Assembly, Pucón, Chile, November, 2004.

Power, J.A., Lahr, J.C., Page, R.A., Chouet, B.A., Stephens, C.D., Harlow, D.H., Murray, T.L., Davies, J.N., 1994. Seismic evolution of the 1989–1990 eruption sequence of Redoubt Volcano, Alaska. J. Volcanol. Geotherm. Res. 62, 69–94.

Power, J.A., Stihler, S.D., White, R.A., Moran, S.C., 2002. Observations of deep long-period (DLP) seismic events beneath Aleutian Arc volcanoes; 1989 to 2002. EOS Trans. Am. Geophys. Union 83 (47) (Fall Meet. Suppl., Abstract S11D-11).

Richter, C.F., 1935. An instrumental earthquake magnitude scale. Bull. Seismol. Soc. Am. 25, 1–32.

Ripepe, M., Gordeev, E., 1999. Gas bubble dynamics model for shallow volcanic tremor at Stromboli. J. Geophys. Res. 104, 10639–10654.

Ripepe, M., Poggi, P., Braun, T., Gordeev, E., 1996. Infrasonic waves and volcanic tremor at Stromboli. Geophys. Res. Lett. 23 (2), 181–184.

Ripepe, M., Ciliberto, S., Schiava Della, M., 2001. Time constraints for modeling source dynamics of volcanic explosions at Stromboli. J. Geophys. Res. 106 (5), 8713–8727.

Stelling, P., Beget, J., Nye, C., Gardner, J., Devine, J.D., George, R.M.M., 2002. Geology and petrology of ejecta from the 1999 eruption of Shishaldin Volcano, Alaska. Bull. Volcanol. 64, 548–561.

Thompson, G., McNutt, S.R., Tytgat, G., 2002. Three distinct regimes of volcanic tremor associated with the eruption of Shishaldin Volcano, Alaska, 1999. Bull. Volcanol. 64, 535–547.

Wessel, P., Smith, W.H.F., 1998. New, improved version of the Generic Mapping Tools released. EOS Trans. Am. Geophys. Union 79, 579.

Zimanowski, B., 1998. Phreatomagmatic Explosions. In: Freund, A., Rosi, M. (Eds.), From Magma to Tephra: Modelling Physical Processes of Explosive Volcanic Eruptions. Elsevier, pp. 25–53.